



## ORIGINAL ARTICLE

# Discovery of novel 1,2,4-triazine-chalcone hybrids as anti-gastric cancer agents via an axis of ROS-ERK-DR5 *in vitro* and *in vivo*



Chong Liu<sup>a,\*</sup>, Jian Song<sup>b,c,1</sup>, Xin-Xin Cui<sup>e,1</sup>, Wen-Bo Liu<sup>a</sup>, Yin-Ru Li<sup>a</sup>,  
Guang-Xi Yu<sup>a</sup>, Xin-Yi Tian<sup>a</sup>, Ya-Feng Wang<sup>b,\*</sup>, Yang Liu<sup>b,\*</sup>,  
Sai-Yang Zhang<sup>a,b,c,d,\*</sup>

<sup>a</sup> Department of Pharmacy, The First Affiliated Hospital of Zhengzhou University, Zhengzhou 450000, China

<sup>b</sup> School of Basic Medical Sciences, Zhengzhou University, Zhengzhou 450001, China

<sup>c</sup> School of Pharmaceutical Sciences, Institute of Drug Discovery & Development, Key Laboratory of Advanced Drug Preparation Technologies (Ministry of Education), Zhengzhou University, Zhengzhou 450001, China

<sup>d</sup> Henan Institute of Advanced Technology, Zhengzhou University, Zhengzhou 450001, China

<sup>e</sup> Department of Pharmacy, Liaocheng People's Hospital, Liaocheng 252000, China

Received 21 October 2021; accepted 13 December 2021

Available online 23 December 2021

## KEYWORDS

1,2,4-Triazine;  
Chalcone;  
Antiproliferative activity;  
ROS;  
ERK;  
DR5

**Abstract** In this work, a series of novel 1,2,4-triazine-chalcone hybrids were designed through the molecular hybridization strategy, synthesized by two step chlorinations and further aldol condensation and evaluated their antiproliferative activity against MGC-803, HCT-116, PC-3, EC-109 and A549 cells. Compound **9I** displayed significant antiproliferative activity against MGC-803, HCT-116, PC-3, EC-109 and A549 cell lines with IC<sub>50</sub> values of 0.41, 0.43, 0.61, 0.78 and 0.52 μM, respectively. Subsequent mechanistic investigations suggested that compound **9I** induced the generation of ROS and inhibited the activation of the ERK pathway. Compound **9I** induced extrinsic cell apoptosis by up-regulating DR5 dependent on the generation of ROS, while up-regulation of DR5 caused by compound **9I** relied on the inhibition of ERK. Thus, compound **9I** inhibited the gastric cancer cells via an axis of ROS-ERK-DR5 *in vitro*. Compound **9I** also showed

\* Corresponding authors at: Department of Pharmacy, The First Affiliated Hospital of Zhengzhou University, Zhengzhou 450000, China (C. Liu, S.-Y. Zhang).

E-mail addresses: liuchong121212@163.com (C. Liu), yfwang@zzu.edu.cn (Y.-F. Wang), liuyang8016@126.com (Y. Liu), saiyangz@zzu.edu.cn (Sai-Yang Zhang).

<sup>1</sup> These authors contributed equally to this work.

Peer review under responsibility of King Saud University.



potent activity on cell proliferation inhibition, and was effective in suppressing the growth of MGC-803 xenograft tumor in nude mice without obvious toxicity. Therefore, compound **9I** is to be reported as anti-gastric cancer agent *in vitro* and *in vivo* via an axis of ROS-ERK-DR5.

© 2021 The Author(s). Published by Elsevier B.V. on behalf of King Saud University. This is an open access article under the CC BY-NC-ND license (<http://creativecommons.org/licenses/by-nc-nd/4.0/>).

## 1. Introduction

Gastric cancer is the fifth most common cancers with over 1,000,000 estimated new cases every year globally and the third most common cause of cancer related deaths, with 784,000 deaths globally in 2018 (Freddie et al., 2018). Perioperative, adjuvant chemotherapy or targeted therapies licensed to treat gastric cancer have apparently improved the survival rate of patients (Ilson, 2017). However, drug resistance and cancer recurrence occurred in more than about 60% of patients receiving treatment (Ilson, 2017). Noteworthy, there are few clinical drugs which can specially inhibit advanced and relapse gastric cancers (Biagioni et al., 2019). Therefore, novel agents targeting gastric cancer are highly desirable and necessary.

Reactive oxygen species (ROS) is an important participant in cellular oxidative stress (Sies and Jones, 2020). ROS affects many physiological behaviors including cell metabolism, survival and death. High levels of ROS cause cell damage, DNA damage and apoptosis by oxidation and nitration of macromolecules including lipids, proteins, RNA and DNA (Sies and Jones, 2020). In addition, the levels of ROS may also affect the activation of related cell signaling pathways such as MAPK (Mitogen-Activated Protein Kinases) (Prasad et al., 2017). MAPK is a conserved tertiary kinase cascade which has a wide range of effects on cells (Rezatabar et al., 2019). As an important member of MAPK, the ERK (Extracellular Regulated Protein Kinases) signaling pathway can regulate cell apoptosis by regulating death receptors. Thus, exploiting the increase of ROS levels in cancer cells has become a novel target strategy to improve therapeutic activity and selectivity in the development of anticancer agents.

Chalcone is a natural product with versatile biological and pharmacological properties especially anticancer activity (Zhuang et al., 2017). Simple chalcones or chalcone hybrids exhibited anticancer activity by the interaction with molecular targets such as ROS; mitochondrial pathway, tubulin, MAPK signaling pathway or JAK/STAT signaling pathway (The Janus Tyrosine Kinase / Signal Transducer and Activator of Transcription) (Mahapatra et al., 2015; Gao et al., 2020; Lu et al., 2020; Guan et al., 2021; Zhang et al., 2016; Fu et al., 2016). Chalcones which induced apoptosis of cancer cells via regulating ROS levels and its related signaling pathways are usually reported as anticancer agents (Zhu et al., 2018; Takac et al., 2020; Zhang et al., 2017; Zhu et al., 2018; Hou et al., 2020; Zhang et al., 2015; Hseu et al., 2012; Ashour et al., 2020; Fu et al., 2019). For example, as shown in Fig. 1, Flavokawain **B** exhibited its anti-proliferative potency against HSC-3 cells (Human oral squamous cell carcinoma cells) via inducing the generation of ROS and down regulating the MAPK signaling pathway (Hseu et al., 2012). 1,2,3-Triazole-chalcone **1** inhibited RPMI-8226 cells (Human multiple myeloma cells) with an IC<sub>50</sub> of 0.49 μM, caused the cell cycle arrest at G2/M phase, induced apoptosis via triggering

mitochondrial apoptotic pathway and inducing the accumulation of ROS (Ashour et al., 2020). Chalcone-dithiocarbamate **2** was reported as a ROS-mediated apoptosis inducer by inhibiting catalase to exert anticancer activity against human prostate carcinoma PC-3 cells (IC<sub>50</sub> = 1.05 μM) (Fu et al., 2019).

1,2,4-Triazine is a common and crucial scaffold which was found in many biologically active compounds with many interesting pharmacological activities including anti-microbial, anti-HIV, anti-inflammatory and anti-cancer activities (Marín-Ocampo et al., 2019; Cascioferro et al., 2017; Bhide et al., 2006; Bernat et al., 2020; Xiang et al., 2020; Megally Abdo et al., 2020; Kuroda et al., 2006; Dao et al., 2017; Song et al., 2020; Fu et al., 2017; Song et al., 2021). As a class of anticancer agents; 1,2,4-triazine compounds exhibited promising therapeutic efficacy and clinical potentials to bind to different biological targets (e.g. receptors, enzymes and signaling pathway) (Cascioferro et al., 2017). In fact, many groups have reported various 1,2,4-triazine derivatives as anticancer agents. 3,6-Disubstituted 1,2,4-triazine **3** was a Wnt signaling pathway inhibitor (IC<sub>50</sub> = 0.106 μM) in human colorectal cancer cell line HCT-96 (Kuroda et al., 2006). 3,5,6-Trisubstituted 1,2,4-triazine **4** potently inhibited the proliferation of human glioma cancer cell line U-87MG and HCT-96 cells with IC<sub>50</sub> values of 13.3 and 0.19 μM. And compound **4** showed moderate inhibitory activity to FAK (IC<sub>50</sub> = 0.23-μM) (Dao et al., 2017). 1,2,4-Triazine-based compound **5** was identified as a neddylation pathway inhibitor which blocked the neddylation and inhibited the activity of NAE (NEDD8-activating enzyme) and exhibited antiproliferative potency against human gastric cancer MGC-803 cells (IC<sub>50</sub> = 8.22 μM) (Song et al., 2020) (Fig. 2). In this work, we continued with our study on 1,2,4-triazine derivatives to discover potent anticancer agents.

Based on the above findings and as a continuation of our studies on chalcone and 1,2,4-triazine derivatives, 1,2,4-triazine scaffold and chalcone fragment were combined through the molecular hybridization strategy to get novel anticancer compounds. Thus, novel 1,2,4-triazine-chalcone derivatives were firstly designed through the molecular hybridization strategy, synthesized and further explored its antiproliferative activity (Fig. 3). Fortunately, the incorporation of a 1,2,4-triazine scaffold into chalcones could significantly improve the antiproliferative ability. Compound **9I** displayed most potent antiproliferative ability against MGC-803 cells with IC<sub>50</sub> values of 0.41 μM. Further mechanistic studies indicated compound **9I** inhibited the gastric cancer cells via an axis of ROS-ERK-DR5 *in vitro* and *in vivo*.

## 2. Chemistry

The chemical synthesis routes of 1,2,4-triazine-chalcone derivatives was outlined in Scheme 1. The starting compound chloride **6** were prepared from 1,2,4-triazine-3,5(2H,4H)-dione

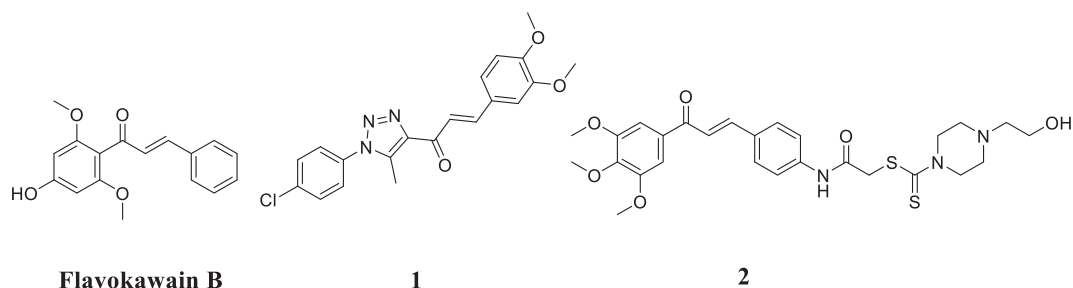


Fig. 1 Structures of reported chalcones with anticancer activity via regulating ROS levels.

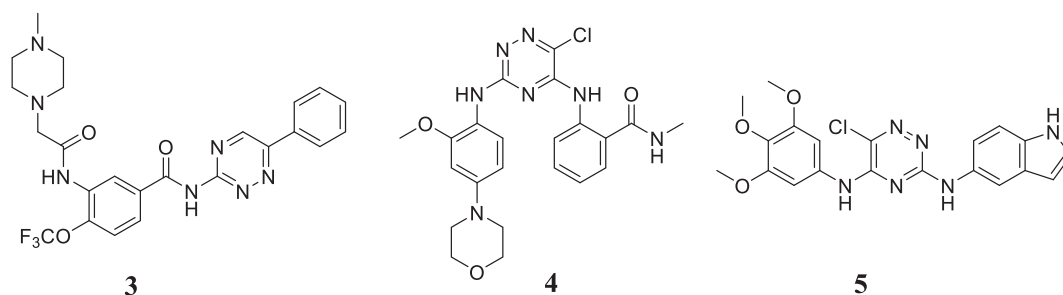


Fig. 2 Structures of reported 1,2,4-triazine derivatives with anticancer activities.

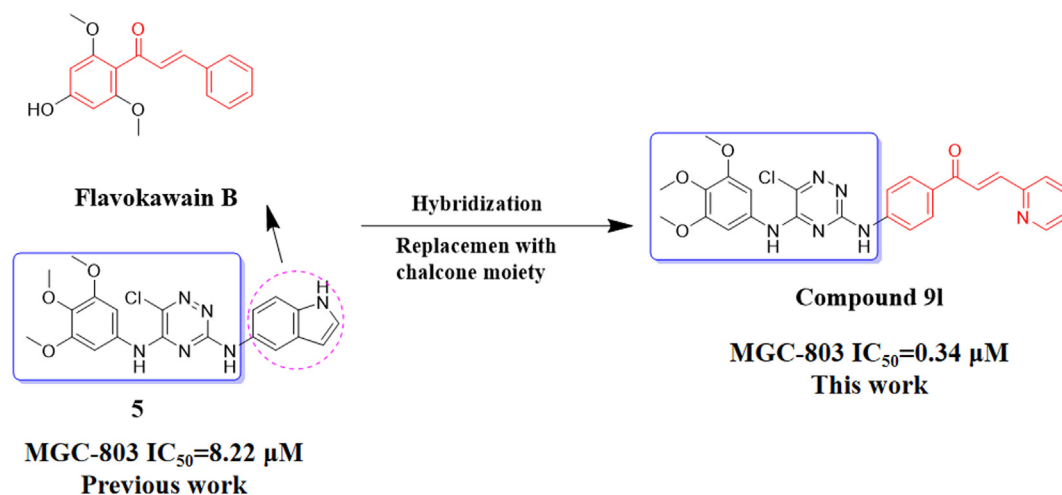


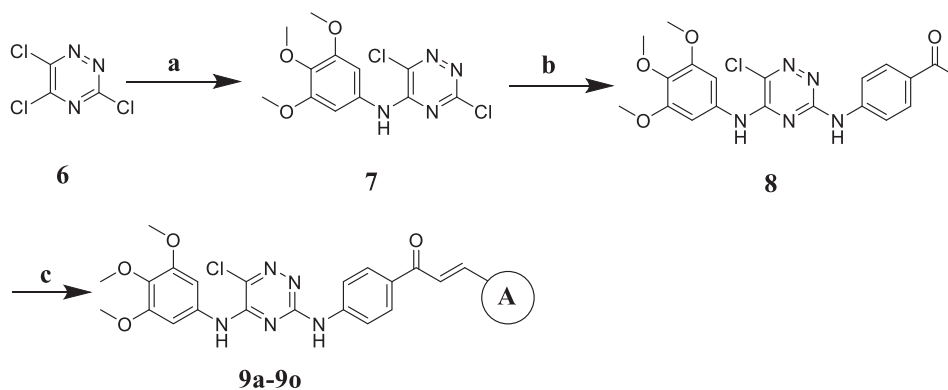
Fig. 3 Design of 1,2,4-triazine-chalcone derivative 9I in this work and the structures of Flavokawain B (Hseu et al., 2012) and compound 5 (Song et al., 2020).

within 2 steps according to the previously reported work (Song et al., 2020). Substitution of compound 6 reacted with the 3,4,5-trimethoxyaniline gave compound 7 in the presence of triethylamine at 65 °C in tetrahydrofuran. Then compound 7 reacted with 4-aminoacetophenone to form compound 8 in the presence of camphor sulfonic acid in isopropanol at 85 °C. Finally, the aldol reactions between compound 8 with different aromatic aldehydes furnished target compounds 9a-9o in ethanol in the presence of sodium hydroxide at 25 °C. Characterization of compounds 9a-9o was carried out by means of NMR and HRMS spectra.

### 3. Biological evaluation

#### 3.1. *In vitro* antiproliferative activity

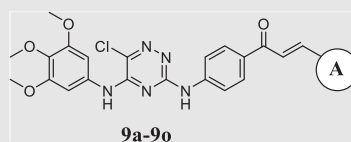
The *in vitro* antiproliferative activities of new target compounds 9a-9o were evaluated against human gastric cancer cell line MGC-803, human colorectal cancer cell line HCT-116, human prostate cancer cell line PC-3, human esophageal cancer cell line EC-109 and human lung cancer cell line A549 using MTT assay and 5-Fluorouracil (5-FU) as the positive



**Reagents and conditions:** a) 3,4,5-trimethoxyaniline, triethylamine, tetrahydrofuran, 65°C. (b) arylamines, trisodium citrate dihydrate, isopropanol, reflux. c) aromatic aldehydes, sodium hydroxide, ethanol, 25 °C.

**Scheme 1** Synthesis of compounds **9a-9o**.

**Table 1** *In vitro* antiproliferative activity of compounds **9a-9o** against human cancer cells.



| Compd.      | Ar   | IC <sub>50</sub> (μM) <sup>a</sup> |                    |                    |                    |                    |
|-------------|--|------------------------------------|--------------------|--------------------|--------------------|--------------------|
|             |  | MGC-803                            | HCT-96             | PC-3               | EC-109             | A549               |
| <b>9a</b>   | phenyl   | 0.95 ± 0.02                        | 0.95 ± 0.08        | 1.81 ± 0.07        | 3.84 ± 0.12        | 2.84 ± 0.9         |
| <b>9b</b>   | 4-F-phenyl                                     | 0.81 ± 0.05                        | 1.01 ± 0.9         | 1.54 ± 0.08        | 6.27 ± 0.14        | 1.46 ± 0.07        |
| <b>9c</b>   | 4-Br-phenyl                                    | 1.88 ± 0.32                        | 2.28 ± 0.34        | 5.64 ± 0.18        | > 10               | 1.47 ± 0.19        |
| <b>9d</b>   | 4-Cl-phenyl                                    | 1.62 ± 0.12                        | 1.91 ± 0.15        | 4.92 ± 0.14        | 3.84 ± 0.12        | 1.47 ± 0.19        |
| <b>9e</b>   | 4-OCH <sub>3</sub> -phenyl                     | 1.55 ± 0.28                        | 1.75 ± 0.31        | 7.21 ± 0.17        | > 10               | 1.03 ± 0.9         |
| <b>9f</b>   | 4-CH <sub>3</sub> -phenyl                      | 0.80 ± 0.18                        | 0.72 ± 0.25        | 1.81 ± 0.07        | 2.91 ± 0.10        | 1.81 ± 0.46        |
| <b>9g</b>   | 3,4,5-(OCH <sub>3</sub> ) <sub>3</sub> -phenyl | 0.54 ± 0.05                        | 0.62 ± 0.08        | 1.24 ± 0.05        | 2.27 ± 0.09        | 0.89 ± 0.03        |
| <b>9h</b>   | 3,4-(OCH <sub>3</sub> ) <sub>2</sub> -phenyl   | 0.92 ± 0.64                        | 1.06 ± 0.12        | 3.48 ± 0.9         | > 10               | > 10               |
| <b>9i</b>   | 3-OH-4-OCH <sub>3</sub> -phenyl                | 0.81 ± 0.08                        | 0.88 ± 0.15        | 0.48 ± 0.04        | 0.79 ± 0.06        | 1.12 ± 0.13        |
| <b>9j</b>   | 3-CH <sub>3</sub> -4-OCH <sub>3</sub> -phenyl  | 1.38 ± 0.20                        | 0.89 ± 0.09        | 0.77 ± 0.02        | > 10               | 1.85 ± 0.12        |
| <b>9k</b>   | 2-thienyl                                      | 3.14 ± 0.72                        | 5.32 ± 0.81        | 3.51 ± 0.16        | > 10               | 4.51 ± 0.21        |
| <b>9l</b>   | 2-pyridyl                                      | <b>0.41 ± 0.03</b>                 | <b>0.43 ± 0.03</b> | <b>0.61 ± 0.07</b> | <b>0.78 ± 0.08</b> | <b>0.52 ± 0.08</b> |
| <b>9m</b>   | 3-pyridyl                                      | 0.43 ± 0.03                        | 0.44 ± 0.02        | 0.52 ± 0.05        | 0.75 ± 0.03        | 0.71 ± 0.02        |
| <b>9n</b>   | 4-pyridyl                                      | 0.44 ± 0.01                        | 0.53 ± 0.02        | 0.77 ± 0.08        | 0.96 ± 0.03        | 0.82 ± 0.08        |
| <b>9o</b>   | 3-OCH <sub>3</sub> -4-pyridyl                  | 0.75 ± 0.01                        | 0.77 ± 0.03        | 1.42 ± 0.06        | 1.04 ± 0.12        | 0.98 ± 0.12        |
| <b>5-Fu</b> | –  | 6.88 ± 1.07                        | 15.8 ± 1.02        | 18.4 ± 1.73        | 10.8 ± 1.52        | 22.7 ± 1.42        |

<sup>a</sup> *In vitro* antiproliferative activity was assayed by exposure for 48 h.

drug. The following **Table 1** depicted the results of *in vitro* antiproliferative activity.

As shown in **Table 1**, most of 1,2,4-triazine-chalcone derivatives exhibited potent antiproliferative potency against MGC-803, HCT-96, PC-3, EC-109 and A549 and obviously better than the positive control drug **5-FU** and compound **5**. Particularly, compound **9l** exhibited the most potent growth inhibitory effects against the tested five human cancer cell lines (MGC-803, HCT-96, PC-3, EC-109 and A549) with IC<sub>50</sub> values of 0.41, 0.43, 0.61, 0.78 and 0.52 μM, respectively. The antiproliferative activities of the compounds varied with respect to its groups on A ring. Most of compounds showed potent antiproliferative potency against four cell lines

(MGC-803, HCT-96, PC-3 and A549) with IC<sub>50</sub> values less than 5.0 μM. And, MGC-803 cells were more sensitive to the compounds than other cancer cells with IC<sub>50</sub> values less than 2.0 μM. Therefore, we discussed the structure-activity relationships of these compounds by using the antiproliferative activity results of MGC-803 cells. Compared compounds **9a** with **9b-9d** and **9e-9j**, compounds **9b-9d** with electron-donating groups at phenyl group of A ring exhibited weaker potency than compounds **9e-9j** with electron-withdrawing groups at phenyl group of A ring and compound **9a** without substituent group at phenyl group of A ring against MGC-803 cells. Therefore, the relationships between the antiproliferative activity of electron-donating groups at A ring and compounds **9a** and

**9e-9j** were 3,4,5-(OCH<sub>3</sub>)<sub>3</sub> > 3-OH-,4-(OCH<sub>3</sub> > 4-CH<sub>3</sub> > 3,4-(OCH<sub>3</sub>)<sub>2</sub> > H > 3-CH<sub>3</sub>-,4-OCH<sub>3</sub> > 4-CH<sub>3</sub>. In addition, the relationships between the antiproliferative activity of electron-withdrawing groups at A ring and compounds **9a** and **9b-9e** were 4-F > H > 4-Cl > 4-Br.

Moreover, aromatic heterocyclic substituent groups of A ring displayed big difference compared with compound **9a**. Compounds **9l-9o** with the pyridyl groups of A ring displayed better antiproliferative activity against five cancer cells with IC<sub>50</sub> values than the compounds with phenyl groups of A ring. But, the thienyl group of A ring (compound **9k**) might significantly impair antiproliferative activity than the compounds **9a-9j** with the phenyl groups of A ring and compounds **9l-9o** with pyridyl groups of A ring. The relationships between the antiproliferative activity of electron-donating groups at A ring and compounds **9a** and **9e-9j** were 2-pyridyl > 3-pyridyl > 4-pyridyl > phenyl groups > thienyl group.

All the results also indicated that the combinations of 1,2,4-triazine scaffold and chalcones were effective to improve the antiproliferative ability and compound **9l** displayed 22-fold antiproliferative potency than compound **5** against MGC-803 cells.

### 3.2. Compound **9l** inhibited gastric cancer cells *in vitro*

For the outstanding antiproliferative activity against gastric cancer cells MGC-803, compound **9l** also was selected to do further researches on another gastric cancer MGC-803 and SGC-7901 cells. As shown in Fig. 4A, compound **9l** inhibited the activity of gastric cancer MGC-803 and SGC-7901 cells in a dose-dependent manner. And, it did not show high toxicity on gastric normal cells GES-1. Compound **9l** also inhibited MGC-803 and SGC-7901 in a time-dependent manner (Fig. 4B, C & D). With the treatment time raising, cell viability was obviously inhibited, and the inhibition rate against MGC-803 and SGC-7901 cells was over 80% in high dose treatment group (Fig. 4B & D). The growth curves of gastric cancer cells were shown in Fig. 4C & E, compound **9l** evidently inhibited gastric cancer cells. The inhibition of gastric cancer cells by compound **9l** induced cell death, nucleus fragment and concentration and morphology changes (Fig. 4F & G).

These results indicated that compound **9l** inhibited gastric cancer MGC-803 and SGC-7901 cells in time and dose-dependent manners.

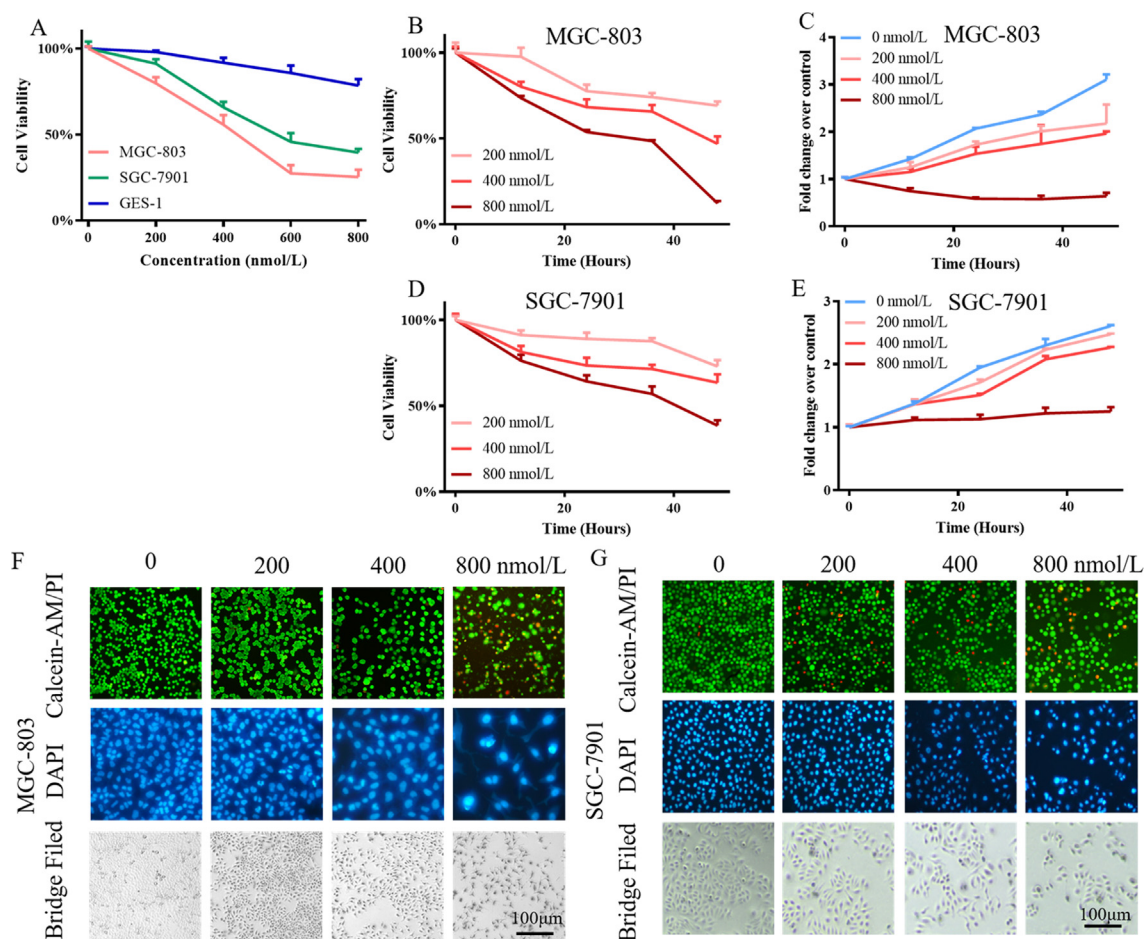


**Fig. 4** Compound **9l** inhibited gastric cancer cells *in vitro*. A, B & D. Cell viability of gastric cancer MGC-803 and SGC-7901 cells after the treatment with indicated concentrations of **9l** for 48 h; C & E. Growth curves of gastric cancer cells after the treatment indicated concentrations of **9l**; F & G. Cell death Avermectin induced (upper panel, dead cells were stained red), cellular morphologies (lower panel) and nucleus (mid panel). Cells were treated with different concentrations of compound **9l** for 48 h, then cells were stained with different dyes.

### 3.3. Compound 9l induced the generation of ROS to inhibit the ERK pathway

One promising anticancer mechanism of chalcones is to modulate the generation of ROS. ROS affects many physiological behaviors including cell metabolism, survival and death. Therefore, the levels of ROS in gastric cancer MGC-803 and SGC-7901 cells after the treatment with compound 9l were detected next. As the concentration of compound 9l raising, compound 9l up-regulated the levels of ROS in gastric cancer cells (Fig. 5A). The increment of ROS may have an influence on the ERK pathway. Therefore, the members of the ERK cascade were detected. As shown in Fig. 5B, C & D, compound 9l inhibited the activation (phosphorylation) of c-Raf, MEK (Mitogen-activated protein kinase) and ERK, which resulted in a decrease of p-P90RSK and c-Myc which were 2 substrates of ERK pathway in gastric cancer MGC-803 and SGC-7901

cells. NAC (N-acetyl-L-cysteine), a well-known antioxidant, could reduce the levels of ROS in cells. In gastric cancer MGC-803 and SGC-7901 cells, NAC evidently reversed the inhibition of the ERK pathway induced by compound 9l (Fig. 5E, F & G).

In summary, compound 9l increased the levels of ROS in gastric cancer MGC-803 and SGC-7901 cells and induced ERK pathway inhibition depending on the ROS increment.

### 3.4. Compound 9l induced cell apoptosis in gastric cancer cells

The cell apoptosis of gastric cancer MGC-803 and SGC-7901 cells were tested after the treatment with compound 9l. The results showed compound 9l induced cell apoptosis in a dose-dependent manner in gastric cancer MGC-803 and SGC-7901 cells (Fig. 6A). As shown in Fig. 6A, after treatment with the 800 nM concentration of compound 9l for 48 h, the

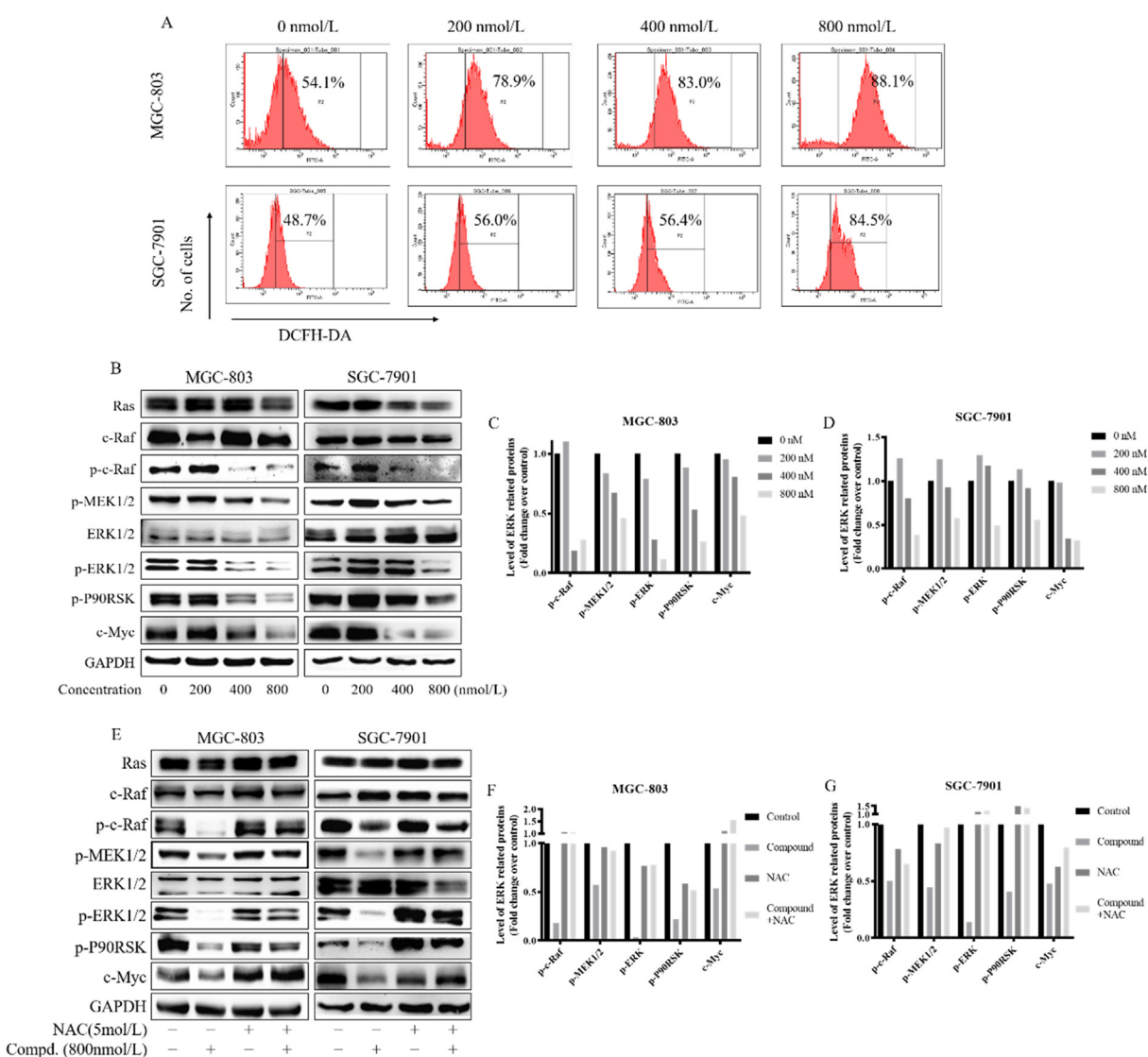


**Fig. 5** Compound 9l inhibited ERK pathway via ROS generation. A. ROS level of gastric cancer MGC-803 and SGC-7901 cells after the treatment with indicated concentrations of 9l; B to G. Levels of ERK pathway related proteins in gastric cancer MGC-803 and SGC-7901 cells. MGC-803 and SGC-7901 cells were treated with different concentrations of compound 9l for 48 h alone, or combine with NAC.

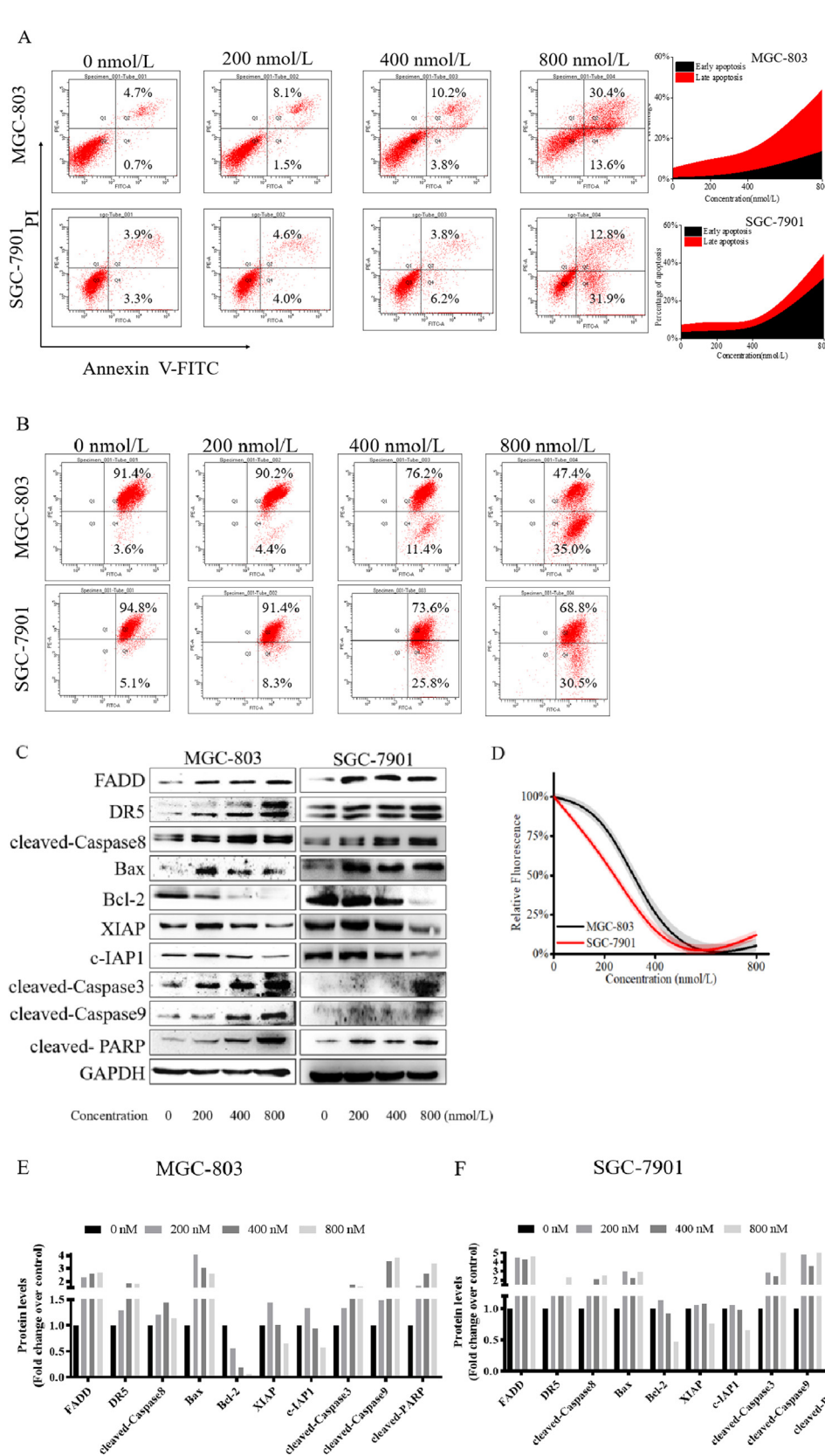


**Fig. 6** Compound **9I** induced cell apoptosis in gastric cancer MGC-803 and SGC-7901 cells. Cells were treated with indicated concentrations of compound **9I** for 48 h. A. Cell apoptosis percentage of gastric cancer MGC-803 and SGC-7901 cells induced by compound **9I**; B & D. Mitochondrial membrane potential ( $\Delta\Psi_m$ ) depolarization of gastric cancer cells induced by compound **9I**; C, E & F. Levels of cell apoptosis related proteins in gastric cancer MGC-803 and SGC-7901 cells.

percentages of total apoptotic cells from 5.4% (0 nM, MGC-803), 7.2% (0 nM, SGC-7901) significantly increased to 44.0% (800 nM, MGC-803), 44.7% (800 nM, SGC-7901) respectively. These results suggested that compound **91** could dose-dependently induce cell apoptosis in MGC-803 and SGC-7901 cells. At the protein levels, the up-regulations of FADD (Fas-associating protein with a novel death domain), DR5 (Death receptor 5), cleaved-Caspase8 indicated that compound **91** induced an extrinsic-apoptosis in gastric cancer MGC-803 and SGC-7901 cells. As the results shown, the intrinsic-apoptosis related pro-apoptosis protein Bax was up-regulated; anti-apoptosis proteins Bcl-2, XIAP (X-linked inhibitor of apoptosis protein), c-IAP1 (Cellular inhibitor of apoptosis protein 1) were down-regulated; Caspase9, Caspase3 and PARP (poly ADP-ribose polymerase) were cleaved (Fig. 6C, E&F, S1, S2). Further studies suggested compound **91** induced depolarization of mitochondrial membrane potential ( $\Delta\Psi_m$ , Fig. 6B & D), which is a marking event of intrinsic-apoptosis. As a result, compound **91** significantly induced

apoptosis in gastric cancer MGC-803 and SGC-7901 cells. Their apoptosis rates both exceeded 44%. To sum up, compound **91** induced extrinsic and intrinsic apoptosis in gastric cancer MGC-803 and SGC-7901 cells.

### 3.5. Compound 91 induced cell apoptosis in gastric cancer cells depending on ROS generation

The generation of ROS usually induces intrinsic apoptosis. To study the relationship between ROS generation and apoptosis induced by compound **91**, further researches were done with NAC. As shown in Fig. 7, NAC reversed the effects of compound **91** on inducing depolarization of mitochondrial membrane potential ( $\Delta\Psi_m$ , Fig. 7A & B), inducing cell apoptosis (Fig. 7C & D), inhibiting cell viability (Fig. 7E) in gastric cancer MGC-803 and SGC-7901 cells. These results indicated that the inducement of cell apoptosis by compound **91** depending on ROS generation. At the protein levels, NAC inhibited the up regulation of DR5, and cleavage of Caspase8, Caspase9, Cas-

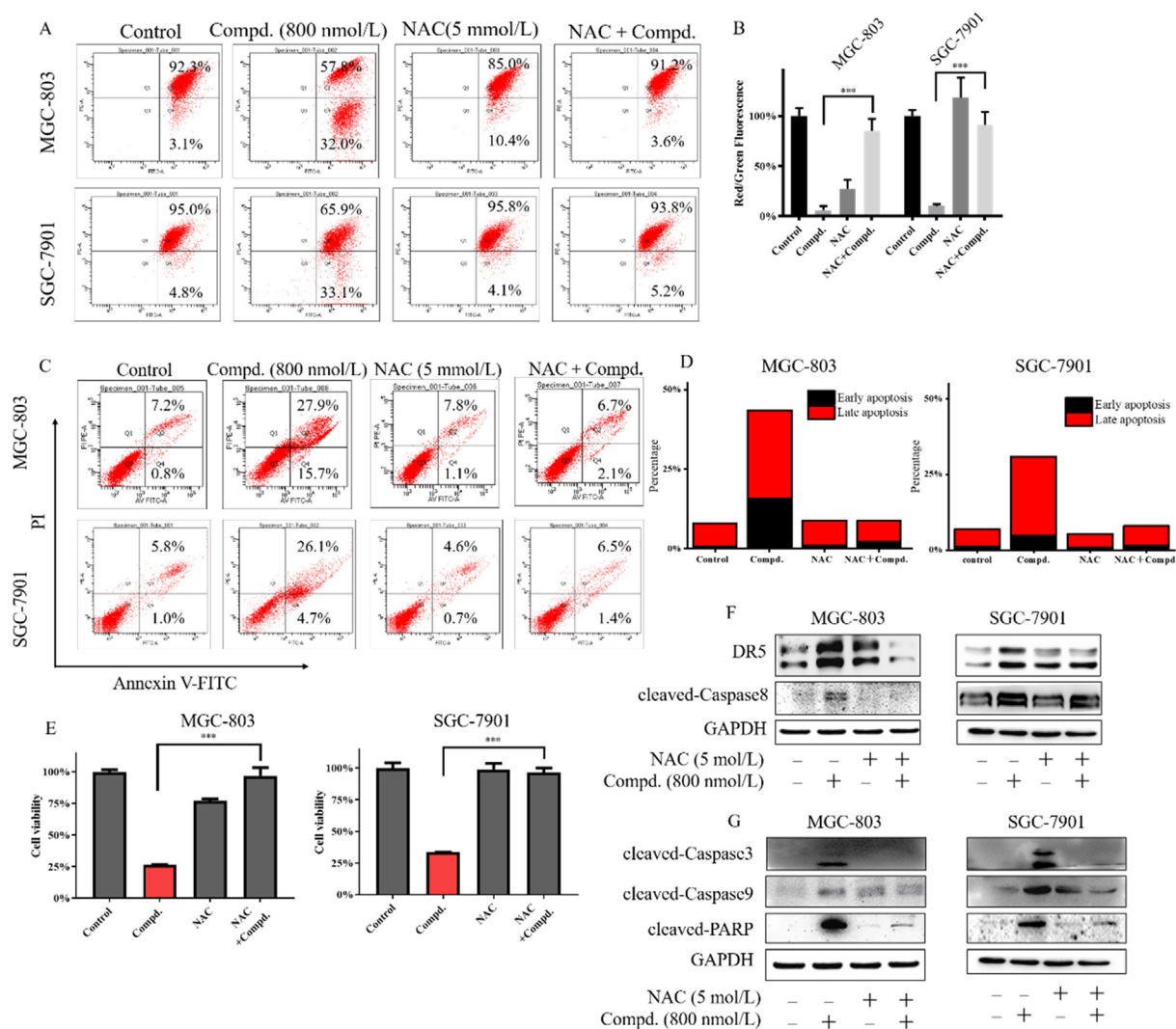


**Fig. 7** Compound **91** induced cell apoptosis via ROS generation, cells were treated with compound **91**, NAC or both compound **91** and NAC for 48 h. A & B. Mitochondrial membrane potential ( $\Delta\Psi_m$ ) depolarization of gastric cancer MGC-803 and SGC-7901 cells; C & D. Cell apoptosis percentage of gastric cancer cells; E. Cell viability of gastric cancer cells after the treatment with compound **91**, NAC or both compound **91** and NAC for 48 h; F & G. Levels of apoptosis related proteins after the treatment with compound **91**, NAC or both compound **91** and NAC for 48 h.

pase3 and PARP induced by compound **91** in gastric cancer MGC-803 and SGC-7901 cells (Fig. 7F & G).

Thus, it indicated that compound **91** induced extrinsic and intrinsic apoptosis in gastric cancer MGC-803 and SGC-7901 cells depending on the generation of ROS.

### 3.6. Compound **91** inhibited gastric cancer cells depending on its effects on *p*-ERK and DR5

The ERK pathway may affect the expression of DR5. In addition, the expression of DR5 could induce cell apoptosis. To

check the necessity of ERK and DR5 existence on the inhibition of gastric cancer cells induced by compound **91**, the RNA interference (siRNA) was used to knock-down ERK/p-ERK (siMAPK1, Fig. S3) and DR5 (siDR5-1, Fig. S4). The knock-down reversed the up-regulation of DR5 and cleavage of PARP induced by compound **91** (Fig. 8 A&B, S5). The cleavage of PARP induced by compound **91** could also be reversed by knockdown of DR5 (Fig. 8 C&D). In the morphology study of the cell nucleus, the knock-down of ERK/p-ERK or DR5 protected the gastric cancer cells from apoptosis-like change induced by compound **91** (Fig. 8 E&F). Briefly, the inhi-

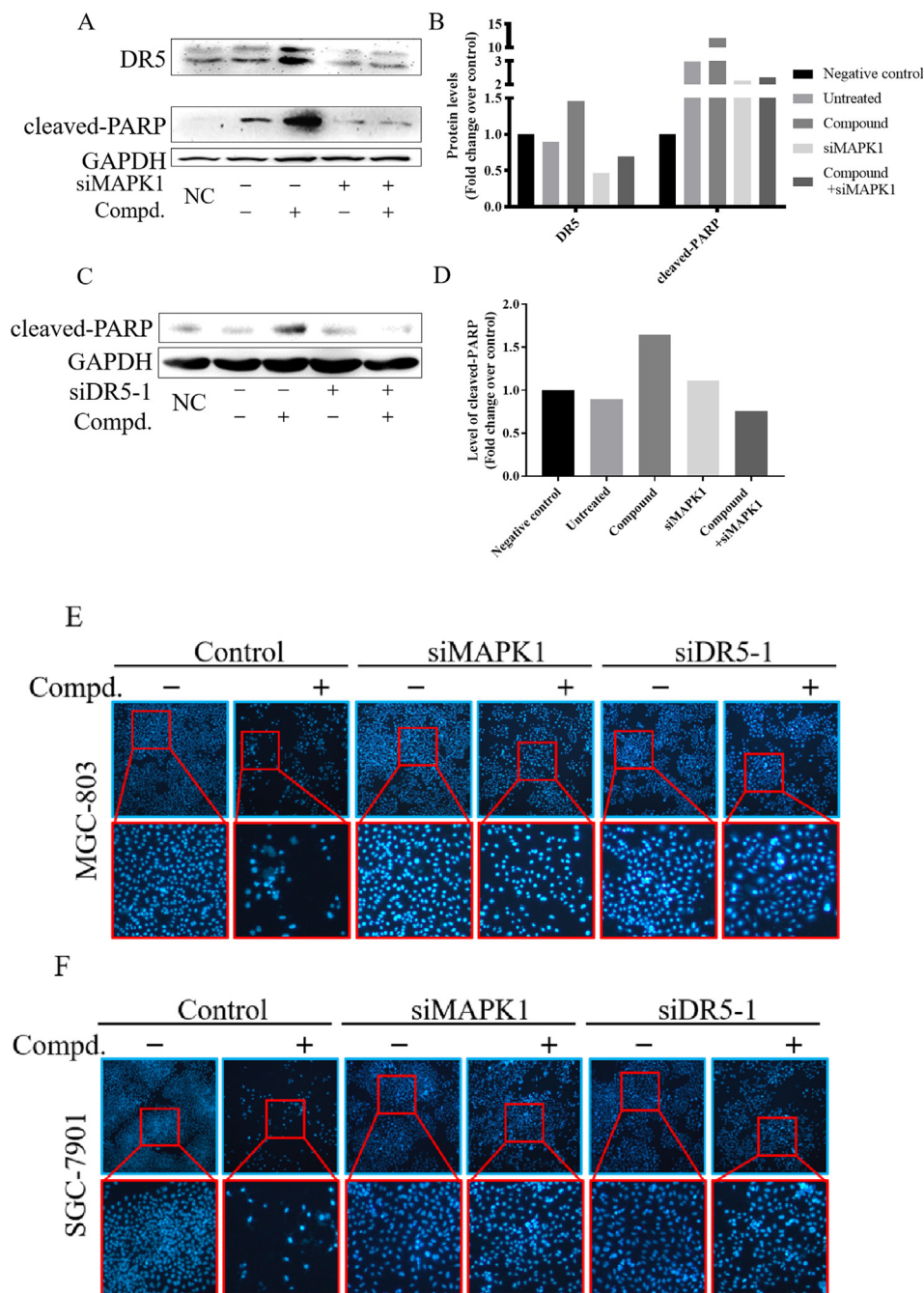


**Fig. 8** Compound **91** inhibited gastric cancer cells via its effect on ERK and DR5. Cells were treated with compound **91** (800 nmol/L) with or without siRNA for ERK or DR5 (100 pmol/L) for 48 h. A, B, C & D. Cell apoptosis related protein levels; E & F. Cell nucleus morphologies of gastric cancer cells.

bition induced by compound **91** on gastric cancer cells depending on the existence of p-ERK and DR5. These results indicated that the up-regulation of DR5 induced by compound **91** depending on the inhibition of the ERK pathway and the cell apoptosis induced by compound **91** depended on the DR5 up-regulation. The cell apoptosis happened via an axis of ROS-ERK-DR5. Therefore, compound **91** induced cell apoptosis via an axis of ROS-ERK-DR5.

### 3.7. Compound **91** inhibited gastric cancer *in vivo*

To verify the anti-cancer activity of compound **91** *in vivo*, the MGC-803 bearing xenograft mice model was established. Models were treated with vehicle control, compound **91** (16,

24 mg/kg) and 5-Fu (positive control, first-line chemotherapy drug of gastric cancers) after tumor volume reached 100 mm<sup>3</sup>. The tumor volume was measured and recorded every other day since the treatment began. As shown in Fig. 9A, compound **91** showed a high inhibition activity on tumor growth. Tumor tissues were collected and measured for their weight after the mice were executed, the tumor weight of compound **91** high-dose treated group was decreased by over 85% (Fig. 9B & E). The further study on tissues showed that the p-ERK, Ki67 was down-regulated and the DR5, cleaved-PARP were up-regulated which were consistent with the *in vitro* results (Fig. 9C, D, G & I). The tissue was tunnel positive after the treatment with compound **91** indicating that the apoptosis was induced by compound **91** (Fig. 9F & H).

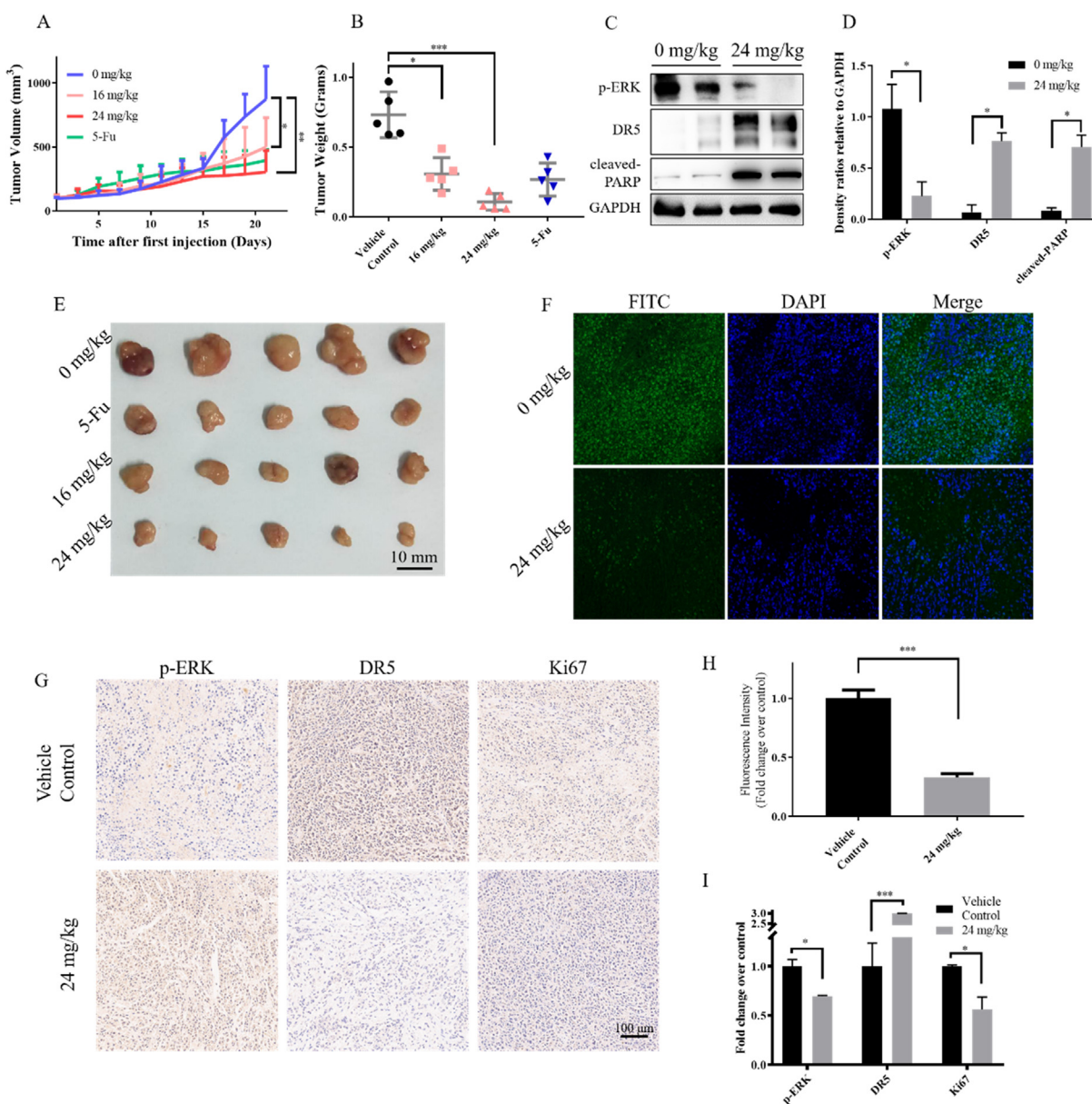


**Fig. 9** Compound **91** inhibited gastric cancer *in vivo*. **A**. Tumor volume during the treatment with compound **91**; **B**. Tumor weight of different groups; **C** & **D**. Protein levels in the tumor tissue; **E**. Pictures of tumor tissue; **F** & **H**. The tunnel level of tumor tissue; **G** & **I**. Level of the p-ERK, DR5 and Ki67 in the tumor tissue.

These results showed compound **9I** inhibited gastric cancer *in vivo*.

### 3.8. Compound **9I** showed no significant toxicity *in vivo*

During the treatment, the animals in the treated group during the treatment did not exhibit differences in motility and activity from the control group. The body weight of mice was measured and recorded every 2 days. Data on Fig. 10 A showed there is no significant difference between vehicle control and treated groups. Blood biochemical indexes related to hepatic and renal function were detected as well, indexes of alanine aminotransferase (ALT), glutamic oxalacetic transaminase (AST), total bilirubin (T-BIL), uric acid (UA), creatinine (CRE), blood urea nitrogen (BUN) did not significantly change (Fig. 10B to G). The H&E staining results also showed on significant toxicity of compound **9I** on the main organs (Fig. 10H).

These results indicated compound **9I** had no significant toxicity *in vivo*.

## 4. Conclusion

Exploiting increased ROS levels and related cell signaling pathways in cancer cells have become a novel target strategy to develop anticancer agents with high therapeutic activity and selectivity. In this work, a series of novel 1,2,4-triazine-chalcone derivatives were designed and synthesized, and their antiproliferative potency on MGC-803, HCT-96, PC-3, EC-109 and A549 cells were evaluated. Compound **9I** exhibited most potent anticancer activities against MGC-803, HCT-96, PC-3, EC-109, and A549 with IC<sub>50</sub> values of 0.41, 0.43, 0.61, 0.78 and 0.52  $\mu$ M, respectively. Therefore, compound **9I** was selected as the key compound for this series.

In the further studies, compound **9I** showed potent activity on inhibiting gastric cancer MGC-803 and SGC-7901 cells (Fig. 4). Compound **9I** could induce the generation of ROS and inhibit the activation of the ERK pathway depending on the generation of ROS (Fig. 5). Compound **9I** induced extrinsic cell apoptosis via up-regulating DR5 (Fig. 6 & Fig. 7). The cell apoptosis induced by compound **9I** also depended on the gen-

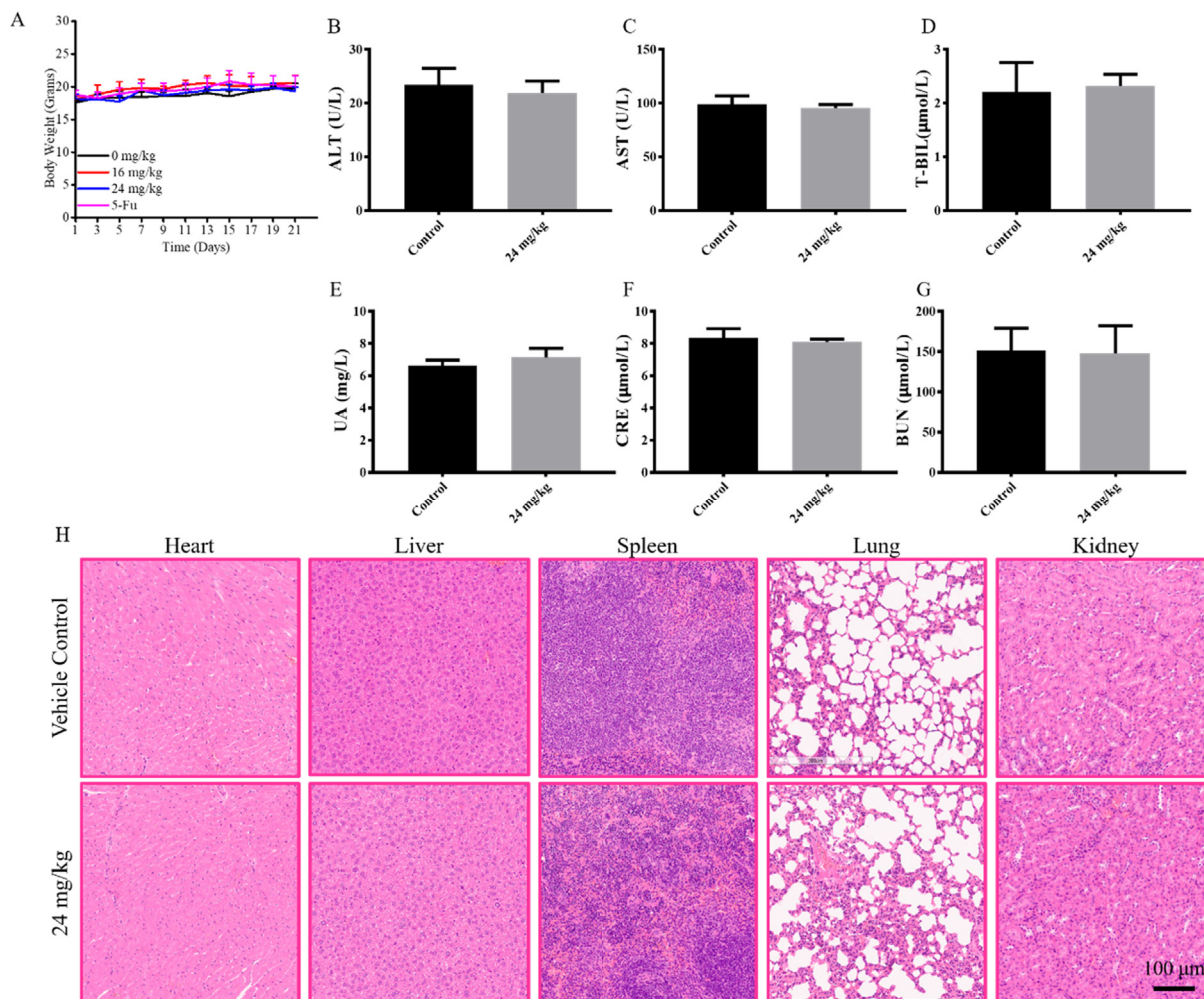


**Fig. 10** Compound **9I** showed no significant toxicity *in vivo*. A. Body weight of mice during the treatment with compound **9I**; B to G. Blood biochemistry indexes; H. H&E staining of mice organs.

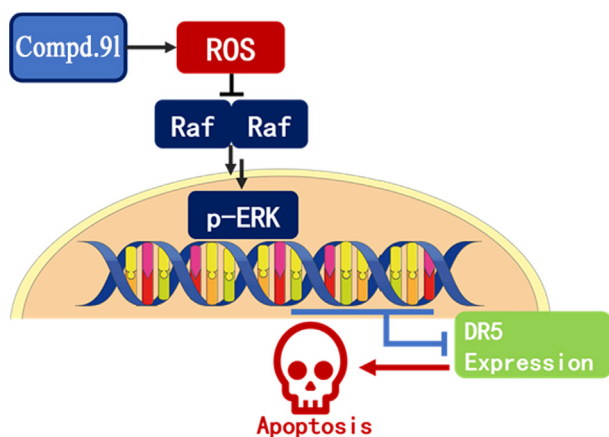


**Fig. 11** Potential mechanism model compound **9I** which activated the ROS-ERK-DR5 axis to inhibit gastric cancers.

eration of ROS (Fig. 7). To detect the causal relationship between the 2 events caused by ROS generation, ERK inhibition and cell apoptosis, ERK and DR5 were knocked down respectively. As shown in Fig. 6, the up-regulation of DR5 caused by compound **9I** relied on the inhibition of ERK. Thus, the compound **9I** inhibited the gastric cancer cells via an axis of ROS-ERK-DR5. The anticancer activity of compound **9I** was verified *in vivo* next (Fig. 9). Compound **9I** was effective in suppressing MGC-803 xenograft tumor growth in nude mice (Fig. 9) with no significant toxicology to the animals (Fig. 10). Besides the activity on cell apoptosis, compound **9I** also showed an activity of cell proliferation inhibition (Fig. S6 to S9).

In summary, compound **9I** is an efficient compound as anticancer agent via an axis of ROS-ERK-DR5 *in vitro* and *in vivo* (Fig. 11). Therefore, we here reported novel 1,2,4-triazine-chalcone derivatives as anticancer agents via an axis of ROS-ERK-DR5 *in vitro* and *in vivo* and the combination of 1,2,4-triazine scaffold and chalcone may offer significant potentiality for the discovery of anticancer agents.

## 5. General information

All the chemical reagents were purchased from commercial suppliers (Energy chemical Company and Zhengzhou He Qi Company). Melting points were determined on an X-5 micromelting apparatus. NMR spectra data was recorded with a Bruker spectrometer.

### 5.1. Synthesis of compound 7

A solution of compound **6** (1.0 mmol), 3,4,5-trimethoxyaniline and triethylamine (2.0 mmol) were added into 20 mL tetrahydrofuran. And the mixture reacted at 65 °C. After 2 h, organic phases were evaporated to get crude products and then were purified to give compound **7** by column chromatography.

#### 3,6-Dichloro-N-(3,4,5-trimethoxyphenyl)-1,2,4-triazin-5-amine (**7**)

Yellow powder, Yield, 51%, m.p. 229–230 °C. <sup>1</sup>H NMR (400 MHz, DMSO *d*<sub>6</sub>) δ 10.09 (s, 1H), 7.06 (s, 2H), 3.77 (s,

6H), 3.68 (s, 3H). <sup>13</sup>C NMR (100 MHz, DMSO *d*<sub>6</sub>) δ 160.08, 152.56, 151.14, 143.40, 135.59, 131.95, 101.87, 60.11, 55.92.

### 5.2. Synthesis of compound 8

A solution of compound **7** (1.0 mmol), 4-aminoacetophenone and camphor sulfonic acid (0.5 eq) were added into isopropanol (20 mL). And the mixture was stirred at 85 °C. After 6 h of reaction, a yellow solid appeared in the solution and filtered to obtain an unpurified crude product and then was purified to give compound **8** by column chromatography.

Yellow powder, Yield, 68%, m.p. 197–198 °C. <sup>1</sup>H NMR (400 MHz, DMSO *d*<sub>6</sub>) δ 9.72 (s, 1H), 9.43 (s, 1H), 7.62 (d, *J* = 8.1 Hz, 2H), 7.18 (t, *J* = 7.6 Hz, 2H), 7.01–6.91 (m, 3H), 3.70 (d, *J* = 11.6 Hz, 9H). <sup>13</sup>C NMR (100 MHz, DMSO *d*<sub>6</sub>) δ 158.39, 152.55, 149.96, 139.72, 135.00, 134.54, 132.86, 128.30, 121.83, 119.33, 102.19, 60.08, 55.78.

### 5.3. Synthesis of compound 9a-9o

A solution of compound **8** (1.0 mmol), aromatic amines (1.0 eq) and NaOH (0.5 eq) were added into ethanol (20 mL). And the mixture was stirred at 25 °C. After 2 h, the solvent was evaporated under vacuum, and the crude residue was purified by silica gel column chromatography to give compound **9a-9o**.

#### (E)-1-(4-((6-chloro-5-((3,4,5-trimethoxyphenyl)amino)-1,2,4-triazin-3-yl) amino) phenyl)-3-phenylprop-2-en-1-one (**9a**)

Yellow powder, Yield, 53%, m.p. 232–234 °C. <sup>1</sup>H NMR (400 MHz, DMSO *d*<sub>6</sub>) δ 10.16 (s, 1H), 9.59 (s, 1H), 8.03 (d, *J* = 8.8 Hz, 2H), 7.84 (ddd, *J* = 27.2, 19.8, 10.7 Hz, 5H), 7.70 (d, *J* = 15.6 Hz, 1H), 7.54–7.39 (m, 3H), 6.99 (s, 2H), 3.73 (d, *J* = 12.0 Hz, 9H). <sup>13</sup>C NMR (101 MHz, DMSO *d*<sub>6</sub>) δ 187.26, 158.06, 152.64, 150.22, 144.60, 142.92, 135.72, 135.31, 134.82, 132.71, 130.70, 130.37, 129.55, 128.88, 128.64, 122.09, 98.27, 102.58, 60.09, 55.89. HR-MS (ESI): Calcd, C<sub>27</sub>H<sub>24</sub>ClN<sub>5</sub>O<sub>4</sub>, [M + H]<sup>+</sup>: 518.1595, found: 518.1594.

#### (E)-1-(4-((6-chloro-5-((3,4,5-trimethoxyphenyl) amino)-1,2,4-triazin-3-yl) amino) phenyl)-3-(4-fluorophenyl) prop-2-en-1-one (**9b**)

Yellow powder, Yield, 38%, m.p. 252–253 °C. <sup>1</sup>H NMR (400 MHz, DMSO *d*<sub>6</sub>) δ 10.13 (d, *J* = 12.8 Hz, 1H), 9.58 (s, 1H), 8.03 (d, *J* = 8.8 Hz, 2H), 7.95 (dd, *J* = 8.7, 5.6 Hz, 2H), 7.89–7.77 (m, 3H), 7.70 (d, *J* = 15.6 Hz, 1H), 7.31 (t, *J* = 8.8 Hz, 2H), 6.98 (d, *J* = 7.0 Hz, 2H), 3.78–3.69 (m, 9H). <sup>13</sup>C NMR (100 MHz, DMSO *d*<sub>6</sub>) δ 187.16, 171.98, 158.05, 152.63, 150.21, 144.61, 141.69, 135.73, 135.25, 132.71, 131.02, 130.93, 130.66, 129.57, 121.98, 98.24, 96.00, 95.78, 102.51, 60.09, 55.86. HR-MS (ESI): Calcd, C<sub>27</sub>H<sub>23</sub>ClFN<sub>5</sub>O<sub>4</sub>, [M + H]<sup>+</sup>: 536.1501, found: 536.1500.

#### (E)-3-(4-bromophenyl)-1-(4-((6-chloro-5-((3,4,5-trimethoxyphenyl)amino)-1,2,4-triazin-3-yl)amino)phenyl)prop-2-en-1-one (**9c**)

Yellow powder, Yield, 34%, m.p. 249–250 °C. <sup>1</sup>H NMR (400 MHz, DMSO *d*<sub>6</sub>) δ 10.12 (s, 1H), 9.58 (s, 1H), 8.06–7.89 (m, 2H), 7.86–7.64 (m, 7H), 6.98 (d, *J* = 7.0 Hz, 3H), 3.74 (s, 6H), 3.71 (s, 3H). <sup>13</sup>C NMR (101 MHz, DMSO *d*<sub>6</sub>) δ 196.10, 158.07, 152.63, 150.23, 144.46, 135.61, 135.27, 132.69, 131.21, 130.99, 130.09, 129.10, 98.02, 102.59, 60.10, 55.86.

**(E)-1-(4-((6-chloro-5-((3,4,5-trimethoxyphenyl) amino)-1,2,4-triazin-3-yl) amino) phenyl)-3-(4-chlorophenyl) prop-2-en-1-one (9d)**

Yellow powder, Yield, 34%, m.p. 250–251 °C. <sup>1</sup>H NMR (400 MHz, DMSO *d*<sub>6</sub>) δ 10.16 (d, *J* = 12.0 Hz, 1H), 9.59 (d, *J* = 9.5 Hz, 1H), 8.02 (d, *J* = 8.9 Hz, 2H), 7.93–7.88 (m, 2H), 7.86–7.79 (m, 2H), 7.73–7.65 (m, 1H), 7.54 (t, *J* = 10.1 Hz, 2H), 7.37 (d, *J* = 14.5 Hz, 1H), 7.00 (d, *J* = 12.1 Hz, 2H), 3.73 (dd, *J* = 16.0, 8.6 Hz, 9H). <sup>13</sup>C NMR (151 MHz, DMSO *d*<sub>6</sub>) δ 187.61, 158.54, 153.13, 150.70, 145.19, 141.96, 135.72, 135.34, 134.30, 133.21, 131.26, 130.86, 130.13, 129.41, 128.77, 123.30, 98.73, 102.98, 60.59, 56.35. HR-MS (ESI): Calcd, C<sub>27</sub>H<sub>23</sub>Cl<sub>2</sub>N<sub>5</sub>O<sub>4</sub>, [M + H]<sup>+</sup>: 552.1205, found: 552.1204.

**(E)-1-(4-((6-chloro-5-((3,4,5-trimethoxyphenyl) amino)-1,2,4-triazin-3-yl) amino) phenyl)-3-(4-methoxyphenyl) prop-2-en-1-one (9e)**

Yellow powder, Yield, 41%, m.p. 230–232 °C. <sup>1</sup>H NMR (400 MHz, DMSO *d*<sub>6</sub>) δ 10.15 (s, 1H), 9.58 (s, 1H), 8.03 (d, *J* = 8.8 Hz, 2H), 7.85 (t, *J* = 9.5 Hz, 4H), 7.67 (d, *J* = 15.5 Hz, 1H), 7.44 (s, 1H), 7.32 (d, *J* = 7.7 Hz, 1H), 7.23 (d, *J* = 7.7 Hz, 1H), 6.99 (s, 2H), 3.90 (s, 3H), 3.75 (s, 6H), 3.71 (s, 3H). <sup>13</sup>C NMR (100 MHz, DMSO *d*<sub>6</sub>) δ 192.80, 158.04, 152.63, 150.28, 143.00, 140.42, 138.22, 136.95, 135.63, 135.26, 132.46, 129.51, 129.9, 128.82, 126.58, 120.98, 98.10, 102.55, 60.10, 55.84, 20.79. HR-MS (ESI): Calcd, C<sub>28</sub>H<sub>26</sub>ClN<sub>5</sub>O<sub>5</sub>, [M + H]<sup>+</sup>: 570.1520, found: 570.1527.

**(E)-1-(4-((6-chloro-5-((3,4,5-trimethoxyphenyl)amino)-1,2,4-triazin-3-yl)amino)phenyl)-3-(p-tolyl)prop-2-en-1-one (9f)**

Yellow powder, Yield, 46%, m.p. 235–236 °C. <sup>1</sup>H NMR (600 MHz, DMSO *d*<sub>6</sub>) δ 10.15 (s, 1H), 9.59 (s, 1H), 8.01 (d, *J* = 8.6 Hz, 1H), 7.76 (ddt, *J* = 47.1, 38.4, 13.7 Hz, 6H), 7.29 (d, *J* = 7.3 Hz, 2H), 6.97 (d, *J* = 25.6 Hz, 2H), 3.75–3.70 (m, 9H), 2.51 (s, 3H). <sup>13</sup>C NMR (100 MHz, DMSO *d*<sub>6</sub>) δ 187.71, 158.56, 153.13, 150.72, 145.02, 143.51, 140.93, 138.72, 137.44, 135.72, 133.22, 132.59, 131.29, 130.16, 130.02, 129.62, 129.33, 129.19, 127.09, 121.46, 98.74, 103.02, 60.59, 56.36, 21.55. HR-MS (ESI): Calcd, C<sub>28</sub>H<sub>26</sub>ClN<sub>5</sub>O<sub>4</sub>, [M + H]<sup>+</sup>: 532.1752, found: 532.1752.

**(E)-1-(4-((6-chloro-5-((3,4,5-trimethoxyphenyl)amino)-1,2,4-triazin-3-yl)amino)phenyl)-3-(3,4,5-trimethoxyphenyl)prop-2-en-1-one (9g)**

Yellow powder, Yield, 47%, m.p. 249–250 °C. <sup>1</sup>H NMR (400 MHz, DMSO *d*<sub>6</sub>) δ 10.16 (s, 1H), 9.58 (s, 1H), 8.04 (d, *J* = 8.8 Hz, 2H), 7.84 (dd, *J* = 12.1, 3.2 Hz, 3H), 7.65 (d, *J* = 15.5 Hz, 1H), 7.21 (s, 2H), 7.00 (s, 2H), 3.88 (s, 6H), 3.75 (s, 6H), 3.73 (s, 3H), 3.70 (s, 3H). <sup>13</sup>C NMR (101 MHz, DMSO *d*<sub>6</sub>) δ 187.18, 158.07, 153.09, 152.64, 150.20, 144.53, 143.39, 139.57, 135.70, 135.26, 132.70, 130.80, 130.37, 129.56, 121.24, 98.21, 106.31, 102.53, 60.9, 56.07, 55.87, 55.60. HR-MS (ESI): Calcd, C<sub>30</sub>H<sub>30</sub>ClN<sub>5</sub>O<sub>7</sub>, [M + H]<sup>+</sup>: 608.1912, found: 608.199.

**(E)-1-(4-((6-chloro-5-((3,4,5-trimethoxyphenyl)amino)-1,2,4-triazin-3-yl)amino)phenyl)-3-(3,4-dimethoxyphenyl)prop-2-en-1-one (9h)**

Yellow powder, Yield, 38%, m.p. 264–265 °C. <sup>1</sup>H NMR (400 MHz, DMSO *d*<sub>6</sub>) δ 10.14 (s, 1H), 9.59 (s, 1H), 8.03 (d, *J* = 8.7 Hz, 2H), 7.80 (dd, *J* = 20.8, 12.1 Hz, 3H), 7.66 (d, *J* = 15.4 Hz, 1H), 7.51 (s, 1H), 7.36 (d, *J* = 8.2 Hz, 1H), 7.06–6.97 (m, 3H), 3.85 (d, *J* = 19.0 Hz, 6H), 3.74 (s, 6H), 3.71 (s, 3H). <sup>13</sup>C NMR (151 MHz, DMSO *d*<sub>6</sub>) δ 187.65, 158.59, 153.16, 151.62, 150.71, 149.53, 144.89, 143.90, 136.16,

135.82, 133.22, 131.52, 129.94, 128.16, 124.08, 120.14, 98.73, 92.12, 91.17, 103.08, 60.60, 56.40, 56.20, 56.10, 40.46, 40.32, 40.18, 40.04, 39.90, 39.76, 39.62. HR-MS (ESI): Calcd, C<sub>29</sub>H<sub>28</sub>ClN<sub>5</sub>O<sub>6</sub>, [M + Na]<sup>+</sup>: 600.1620, found: 600.1627.

**(E)-1-(4-((6-chloro-5-((3,4,5-trimethoxyphenyl)amino)-1,2,4-triazin-3-yl)amino)phenyl)-3-(3-hydroxy-4-methoxyphenyl)prop-2-en-1-one (9i)**

Yellow powder, Yield, 32%, m.p. 270–271 °C. <sup>1</sup>H NMR (400 MHz, DMSO *d*<sub>6</sub>) δ 10.12 (s, 1H), 9.57 (s, 1H), 9.15 (s, 1H), 7.99 (d, *J* = 8.2 Hz, 2H), 7.81 (d, *J* = 8.2 Hz, 2H), 7.61 (d, *J* = 7.9 Hz, 2H), 7.27 (d, *J* = 12.5 Hz, 2H), 7.01 (d, *J* = 9.7 Hz, 3H), 3.85 (s, 3H), 3.75 (s, 6H), 3.73 (s, 3H). <sup>13</sup>C NMR (101 MHz, DMSO *d*<sub>6</sub>) δ 187.16, 157.99, 152.63, 150.25, 150.13, 146.61, 144.28, 143.48, 135.25, 132.68, 131.03, 129.35, 127.70, 121.80, 99.31, 98.28, 94.63, 91.91, 102.54, 60.9, 55.85, 55.65. HR-MS (ESI): Calcd, C<sub>28</sub>H<sub>26</sub>ClN<sub>5</sub>O<sub>6</sub>, [M + Na]<sup>+</sup>: 586.1464, found: 586.1471.

**(E)-1-(4-((6-chloro-5-((3,4,5-trimethoxyphenyl)amino)-1,2,4-triazin-3-yl)amino)phenyl)-3-(4-methoxy-3-methylphenyl)prop-2-en-1-one (9j)**

Yellow powder, Yield, 37%, m.p. 248–249 °C. <sup>1</sup>H NMR (400 MHz, DMSO *d*<sub>6</sub>) δ 10.14 (s, 1H), 9.59 (s, 1H), 8.00 (d, *J* = 8.8 Hz, 2H), 7.81 (dd, *J* = 8.7, 2.3 Hz, 4H), 7.71 (d, *J* = 16.2 Hz, 1H), 7.08–6.92 (m, 4H), 3.83 (s, 3H), 3.73 (d, *J* = 10.5 Hz, 9H). <sup>13</sup>C NMR (151 MHz, DMSO *d*<sub>6</sub>) δ 187.64, 161.68, 158.57, 153.13, 150.71, 144.88, 143.43, 136.16, 135.72, 133.22, 131.70, 131.46, 131.02, 129.91, 127.93, 99.99, 98.73, 94.88, 94.13, 103.01, 60.60, 56.35, 55.85, 55.61. HR-MS (ESI): Calcd, C<sub>29</sub>H<sub>28</sub>ClN<sub>5</sub>O<sub>5</sub>, [M + H]<sup>+</sup>: 562.1852, found: 562.19.

**(E)-1-(4-((6-chloro-5-((3,4,5-trimethoxyphenyl)amino)-1,2,4-triazin-3-yl)amino)phenyl)-3-(thiophen-2-yl)prop-2-en-1-one (9k)**

Yellow powder, Yield, 38%, m.p. 254–255 °C. <sup>1</sup>H NMR (400 MHz, DMSO *d*<sub>6</sub>) δ 10.20 (s, 1H), 9.65 (s, 1H), 7.93 (t, *J* = 14.0 Hz, 3H), 7.86–7.75 (m, 4H), 7.65 (d, *J* = 3.2 Hz, 1H), 7.51 (d, *J* = 15.3 Hz, 1H), 7.19 (dd, *J* = 5.0, 3.7 Hz, 1H), 7.13 (s, 1H), 6.98 (s, 2H), 3.75 (t, *J* = 6.6 Hz, 9H). <sup>13</sup>C NMR (151 MHz, DMSO *d*<sub>6</sub>) δ 187.14, 158.51, 153.16, 150.78, 145.03, 140.37, 136.26, 135.87, 133.19, 132.98, 131.12, 130.51, 129.85, 129.16, 120.82, 98.80, 103.20, 60.63, 56.41. HR-MS (ESI): Calcd, C<sub>25</sub>H<sub>22</sub>ClN<sub>5</sub>O<sub>4</sub>S, [M + H]<sup>+</sup>: 524.959, found: 524.959.

**(E)-1-(4-((6-chloro-5-((3,4,5-trimethoxyphenyl)amino)-1,2,4-triazin-3-yl)amino)phenyl)-3-(pyridin-2-yl)prop-2-en-1-one (9l)**

Yellow powder, Yield, 32%, m.p. 216–217 °C. <sup>1</sup>H NMR (400 MHz, DMSO *d*<sub>6</sub>) δ 10.23 (s, 1H), 9.63 (s, 1H), 8.72 (d, *J* = 4.4 Hz, 1H), 8.15 (d, *J* = 15.4 Hz, 1H), 7.97 (dd, *J* = 12.1, 9.0 Hz, 4H), 7.84 (d, *J* = 8.8 Hz, 2H), 7.69 (d, *J* = 15.4 Hz, 1H), 7.53–7.45 (m, 1H), 6.99 (s, 2H), 3.75 (s, 6H), 3.73 (s, 3H). <sup>13</sup>C NMR (101 MHz, DMSO *d*<sub>6</sub>) δ 187.42, 158.08, 152.61, 150.29, 144.21, 142.03, 137.21, 136.65, 135.29, 133.22, 132.64, 129.89, 129.55, 129.22, 124.84, 122.73, 98.30, 97.90, 102.73, 60.10, 55.79. HR-MS (ESI): Calcd, C<sub>26</sub>H<sub>23</sub>ClN<sub>6</sub>O<sub>4</sub>, [M + H]<sup>+</sup>: 519.1548, found: 519.1547.

**(E)-1-(4-((6-chloro-5-((3,4,5-trimethoxyphenyl)amino)-1,2,4-triazin-3-yl)amino)phenyl)-3-(pyridin-3-yl)prop-2-en-1-one (9m)**

Yellow powder, Yield, 42%, m.p. 262–264 °C. <sup>1</sup>H NMR (400 MHz, DMSO *d*<sub>6</sub>) δ 10.16 (s, 1H), 9.60 (s, 1H), 9.00 (s, 1H), 8.61 (d, *J* = 4.5 Hz, 1H), 8.32 (d, *J* = 8.1 Hz, 1H), 8.03 (dd, *J* = 12.2, 7.7 Hz, 3H), 7.83 (d, *J* = 8.8 Hz, 2H), 7.72 (d, *J* = 15.7 Hz, 1H), 7.50 (dd, *J* = 7.9, 4.8 Hz, 1H),

6.99 (s, 2H), 3.74 (d,  $J = 3.8$  Hz, 6H), 3.71 (s, 3H).  $^{13}\text{C}$  NMR (101 MHz, DMSO  $d_6$ )  $\delta$  191.94, 157.99, 152.63, 150.29, 149.65, 149.05, 145.02, 135.89, 135.29, 134.37, 132.66, 132.61, 131.20, 129.72, 129.53, 129.37, 123.28, 98.15, 102.64, 60.9, 55.83. HR-MS (ESI): Calcd,  $\text{C}_{26}\text{H}_{23}\text{ClN}_6\text{O}_4$ ,  $[\text{M} + \text{H}]^+$ : 519.1548, found: 519.1549.

**(E)-1-(4-((6-chloro-5-((3,4,5-trimethoxyphenyl)amino)-1,2,4-triazin-3-yl)amino)phenyl)-3-(pyridin-4-yl)prop-2-en-1-one (9n)**

Yellow powder, Yield, 44%, m.p. 243–244 °C.  $^1\text{H}$  NMR (400 MHz, DMSO  $d_6$ )  $\delta$  10.19 (s, 1H), 9.61 (s, 1H), 8.67 (d,  $J = 4.5$  Hz, 1H), 8.50 (dd,  $J = 23.7, 15.5$  Hz, 1H), 8.07 (dd,  $J = 22.7, 12.0$  Hz, 2H), 7.82 (dd,  $J = 13.9, 9.1$  Hz, 3H), 7.78–7.60 (m, 2H), 7.28 (dd,  $J = 31.7, 4.7$  Hz, 1H), 6.99–6.94 (m, 2H), 3.75–3.68 (m, 9H).  $^{13}\text{C}$  NMR (151 MHz, DMSO  $d_6$ )  $\delta$  187.60, 158.52, 153.13, 150.81, 150.20, 145.48, 143.19, 142.47, 140.50, 135.73, 134.72, 133.19, 132.48, 130.33, 126.93, 123.42, 122.88, 98.75, 103.01, 60.59, 56.36. HR-MS (ESI): Calcd,  $\text{C}_{26}\text{H}_{23}\text{ClN}_6\text{O}_4$ ,  $[\text{M} + \text{Na}]^+$ : 541.1367, found: 541.1362.

**(E)-1-(4-((6-chloro-5-((3,4,5-trimethoxyphenyl)amino)-1,2,4-triazin-3-yl)amino)phenyl)-3-(6-methoxy-pyridin-3-yl)prop-2-en-1-one (9o)**

Yellow powder, Yield, 28%, m.p. 249–250 °C.  $^1\text{H}$  NMR (400 MHz, DMSO  $d_6$ )  $\delta$  10.24 (s, 1H), 9.62 (s, 1H), 8.08 (d,  $J = 15.2$  Hz, 1H), 7.95 (d,  $J = 8.8$  Hz, 2H), 7.86–7.77 (m, 4H), 7.71 (s, 1H), 7.62 (d,  $J = 15.1$  Hz, 1H), 7.40 (d,  $J = 7.2$  Hz, 1H), 6.98 (s, 2H), 4.01 (s, 3H), 3.75 (s, 6H), 3.70 (s, 3H).  $^{13}\text{C}$  NMR (151 MHz, DMSO  $d_6$ )  $\delta$  187.87, 163.67, 158.60, 153.17, 150.82, 145.29, 142.08, 140.41, 135.82, 133.19, 130.94, 129.98, 125.12, 99.68, 98.75, 93.13, 103.23, 60.59, 56.38, 53.49. HR-MS (ESI): Calcd,  $\text{C}_{27}\text{H}_{25}\text{ClN}_6\text{O}_5$ ,  $[\text{M} + \text{Na}]^+$ : 571.1473, found: 571.1479.

#### 5.4. Cell culture

Five human cancer cell line and GES-1 cells used were cultured in humidified incubator at 37 °C and 5%  $\text{CO}_2$ . The RPMI-1640 medium was supplemented with 10% fetal bovine serum, penicillin (100 U/mL) and streptomycin (0.1 mg/mL).

#### 5.5. MTT assay

Five human cancer cell line and GES-1 cells were seeded into 96-well plates and incubated for 24 h. Then cells were treated with different concentrations of compounds. MTT reagent (20  $\mu\text{L}$  per well) was added after another 48 h, and then the cells were incubated at 37 °C for 4 h. Formazan was then dissolved with DMSO. Absorbencies of formazan solution were measured at 490 nm. The  $\text{IC}_{50}$  values of tested compounds were calculated by SPSS version 17.0.

#### 5.6. Western blotting analysis

Gastric cancer MGC-803 and SGC-7901 cells were seeded in dishes and treated with compound **10** **1** or DMSO. After 48 h, MGC-803 and SGC-7901 cells were collected and then lysed. The denatured lysates of each groups were electrophoretic separated in SDS-PAGE. Proteins were then transferred onto PVDF membranes from gels. After blocking for 2 h, membranes were incubated with primary antibodies

conjugation. Then, the membranes were washed and incubated with 2nd antibodies. At last, specific proteins were detected.

#### 5.7. Xenograft studies

A human gastric cancer subcutaneous transplantation tumor model was established with MGC-803 cells in nude mice (BALB/c-nu, female, 6–8 weeks). After the tumor volume reaches 100  $\text{mm}^3$  the MGC-803 bearing mice were randomized into 3 groups and intraperitoneal injection with normal saline or drugs daily for 21 days. Tumor volume was measured every 2 days ( $\text{Length} \times \text{Width}^2/2$ ). Mice were executed after treatment. 500  $\mu\text{L}$  blood samples was collected each mouse, samples were then centrifuged at 2000 g for 10 min for biochemistry analysis. Tumor and organs tissues were harvested for H&E staining or immunochemistry detection. The experiments in the study were performed comply with the protocols approved by the Institutional Animal Care and Use Committee, Zhengzhou University.

#### 5.8. General methods

In this work, some other assays including colony formation assay, cell apoptosis assay and immunostaining assay were referred to our previous work (Fu et al., 2017; Song et al., 2020; Jian et al., 2019).

In this work, some other assays including colony formation assay, cell apoptosis assay and immunostaining assay were referred to our previous work.

#### Declaration of Competing Interest

The authors declare that they have no known competing financial interests or personal relationships that could have appeared to influence the work reported in this paper.

#### Acknowledgement

This work was supported by the National Natural Sciences Foundations of China (U2004123 for Sai-Yang Zhang). Henan Association of Science and Technology (No. 2020HYTP056 for Sai-Yang Zhang, China) and Science and Technology Department of Henan Province (No. 20202310144, for Sai-Yang Zhang, China). The open fund of state key laboratory of Pharmaceutical Biotechnology, Nanjing University, China (Grant no. KF-GN-202101).

#### Appendix A. Supplementary material

The supporting information provided the date of NMR and HRMS spectra of target compounds. Supplementary data to this article can be found online at <https://doi.org/10.1016/j.arabjc.2021.103644>.

#### References

- Ashour, H.F., Abou-zeid, L.A., El-Sayed, M.A.A., Selim, K.B., 2020. 1,2,3-Triazole-Chalcone hybrids: Synthesis, in vitro cytotoxic activity and mechanistic investigation of apoptosis induction in multiple myeloma RPMI-8226. *Eur. J. Med. Chem.* 189, 112062.

- Bernat, Z., Szymanowska, A., Kciuk, M., Kotwica-Mojzych, K., Mojzych, M., 2020. Review of the Synthesis and Anticancer Properties of Pyrazolo[4,3-e][1,2,4]triazine Derivatives. *Molecules* 25.
- Bhide, R.S., Cai, Z.-W., Zhang, Y.-Z., Qian, L., Wei, D., Barbosa, S., Lombardo, L.J., Borzilleri, R.M., Zheng, X., Wu, L.I., Barrish, J.C., Kim, S.-H., Leavitt, K., Mathur, A., Leith, L., Chao, S., Wautlet, B., Mortillo, S., Jeyaseelan, R., Kukral, D., Hunt, J.T., Kamath, A., Fura, A., Vyas, V., Marathe, P., D'Arienzo, C., Derbin, G., Fargnoli, J., 2006. Discovery and Preclinical Studies of (R)-1-(4-(4-Fluoro-2-methyl-1H-indol-5-yloxy)-5-methylpyrrolo[2,1-f][1,2,4]triazin-6-yloxy)propan-2-ol (BMS-540215), an In Vivo Active Potent VEGFR-2 Inhibitor. *J. Med. Chem.* 49, 2143–2146.
- Biagioni, A., Skalamera, I., Peri, S., Schiavone, N., Cianchi, F., Giommoni, E., Magnelli, L., Papucci, L., 2019. Update on gastric cancer treatments and gene therapies. *Cancer Metastasis Rev.* 38, 537–548.
- Cascioferro, S., Parrino, B., Spanò, V., Carbone, A., Montalbano, A., Barraja, P., Diana, P., Cirrincione, G., 2017. An overview on the recent developments of 1,2,4-triazine derivatives as anticancer compounds. *Eur. J. Med. Chem.* 142, 328–375.
- Dao, P., Lietha, D., Etheve-Quellejeu, M., Garbay, C., Chen, H., 2017. Synthesis of novel 1,2,4-triazine scaffold as FAK inhibitors with antitumor activity. *Bioorg. Med. Chem. Lett.* 27, 1727–1730.
- Freddie, Bray, Jacques, Ferlay, Isabelle, Soerjomataram, Rebecca, Siegel, Lindsey, 2018. Global cancer statistics 2018: GLOBOCAN estimates of incidence and mortality worldwide for 36 cancers in 185 countries, CA: Cancer J. Clinicians.
- Fu, D.J., Li, J.H., Yang, J.J., Li, P., Zhang, Y.B., Liu, S., Li, Z.R., Zhang, S.Y., 2019. Discovery of novel chalcone-dithiocarbamates as ROS-mediated apoptosis inducers by inhibiting catalase. *Bioorg. Chem.* 86, 375–385.
- Fu, D.-J., Zhang, S.-Y., Liu, Y.-C., Zhang, L., Liu, J.-J., Song, J., Zhao, R.-H., Li, F., Sun, H.-H., Liu, H.-M., Zhang, Y.-B., 2016. Design, synthesis and antiproliferative activity studies of novel dithiocarbamate-chalcone derivatives. *Bioorg. Med. Chem. Lett.* 26, 3918–3922.
- Fu, D.-J., Song, J., Hou, Y.-H., Zhao, R.-H., Li, J.-H., Mao, R.-W., Yang, J.-J., Li, P., Zi, X.-L., Li, Z.-H., Zhang, Q.-Q., Wang, F.-Y., Zhang, S.-Y., Zhang, Y.-B., Liu, H.-M., 2017. Discovery of 5,6-diaryl-1,2,4-triazines hybrids as potential apoptosis inducers. *Eur. J. Med. Chem.* 138, 1076–1088.
- Gao, F., Huang, G., Xiao, J., 2020. Chalcone hybrids as potential anticancer agents: Current development, mechanism of action, and structure-activity relationship. *Med. Res. Rev.* 40.
- Guan, Y.-F., Liu, X.-J., Yuan, X.-Y., Liu, W.-B., Li, Y.-R., Yu, G.-X., Tian, X.-Y., Zhang, Y.-B., Song, J., Li, W., Zhang, S.-Y., 2021. Design, Synthesis, and Anticancer Activity Studies of Novel Quinoline-Chalcone Derivatives. *Molecules* 26, 4899.
- Hou, Q., Lin, X., Lu, X., Bai, C., Wei, H., Luo, G., Xiang, H., 2020. Discovery of novel steroidal-chalcone hybrids with potent and selective activity against triple-negative breast cancer. *Bioorg. Med. Chem.* 28, 115763.
- Hseu, Y.-C., Lee, M.-S., Wu, C.-R., Cho, H.-J., Lin, K.-Y., Lai, G.-H., Wang, S.-Y., Kuo, Y.-H., Senthil Kumar, K.J., Yang, H.-L., 2012. The Chalcone Flavokawain B Induces G2/M Cell-Cycle Arrest and Apoptosis in Human Oral Carcinoma HSC-3 Cells through the Intracellular ROS Generation and Downregulation of the Akt/p38 MAPK Signaling Pathway. *J. Agric. Food. Chem.* 60, 2385–2397.
- Ibson, D.H., 2017. Advances in the treatment of gastric cancer, Current Opinion. *Gastroenterology* 33, 473–476.
- Jian, S., Gao, Q.L., Wu, B.W., Li, D., Shi, L., Zhu, T., Lou, J.F., Jin, C.Y., Zhang, Y.B., Zhang, S.Y., Liu, H.M., 2019. Novel tertiary sulfonamide derivatives containing benzimidazole moiety as potent anti-gastric cancer agents: Design, synthesis and SAR studies. *Eur. J. Med. Chem.* 183, 111731.
- Kuroda, T., Rabkin, S.D., Martuza, R.L., 2006. Effective treatment of tumors with strong beta-catenin/T-cell factor activity by transcriptionally targeted oncolytic herpes simplex virus vector. *Cancer Res.* 66, 10127–10135.
- Lu, C.-F., Wang, S.-H., Pang, X.-J., Zhu, T., Li, H.-L., Li, Q.-R., Li, Q.-Y., Gu, Y.-F., Mu, Z.-Y., Jin, M.-J., Li, Y.-R., Hu, Y.-Y., Zhang, Y.-B., Song, J., Zhang, S.-Y., 2020. Synthesis and Biological Evaluation of Amino Chalcone Derivatives as Antiproliferative Agents. *Molecules* 25, 5530.
- Mahapatra, D.K., Bharti, S.K., Asati, V., 2015. Anti-cancer chalcones: Structural and molecular target perspectives. *Eur. J. Med. Chem.* 98, 69–114.
- Marín-Ocampo, L., Veloza, L.A., Abonia, R., Sepúlveda-Arias, J.C., 2019. Anti-inflammatory activity of triazine derivatives: A systematic review. *Eur. J. Med. Chem.* 162, 435–447.
- Megally Abdo, N.Y., Milad Mohareb, R., Halim, P.A., 2020. Uses of cyclohexane-1,3-dione for the synthesis of 1,2,4-triazine derivatives as anti-proliferative agents and tyrosine kinases inhibitors. *Bioorg. Chem.* 97, 103667.
- Prasad, S., Gupta, S.C., Tyagi, A.K., 2017. Reactive oxygen species (ROS) and cancer: Role of antioxidative nutraceuticals. *Cancer Lett.* 387, 95–105.
- Rezatabar, S., Karimian, A., Rameshknia, V., Parsian, H., Majidinia, M., Kofi, T.A., Bishayee, A., Sadeghinia, A., Yousefi, M., Monirialamdari, M., Yousefi, B., 2019. RAS/MAPK signaling functions in oxidative stress, DNA damage response and cancer progression. *J. Cell. Physiol.*
- Sies, H., Jones, D.P., 2020. Reactive oxygen species (ROS) as pleiotropic physiological signalling agents. *Nat. Rev. Mol. Cell Biol.* 21, 363–383.
- Song, J., Cui, X.-X., Wu, B.-W., Li, D., Wang, S.-H., Shi, L., Zhu, T., Zhang, Y.-B., Zhang, S.-Y., 2020. Discovery of 1,2,4-triazine-based derivatives as novel neddylation inhibitors and anticancer activity studies against gastric cancer MGC-803 cells. *Bioorg. Med. Chem. Lett.* 30, 126791.
- Song, J., Gao, Q.L., Wu, B.W., Zhu, T., Cui, X.X., Jin, C.J., Wang, S. Y., Wang, S.H., Fu, D.J., Liu, H.M., Zhang, S.Y., Zhang, Y.B., Li, Y.C., 2020. Discovery of tertiary amide derivatives incorporating benzothiazole moiety as anti-gastric cancer agents in vitro via inhibiting tubulin polymerization and activating the Hippo signaling pathway. *Eur. J. Med. Chem.* 203, 112618.
- Song, J., Liu, Y., Yuan, X.-Y., Liu, W.-B., Li, Y.-R., Yu, G.-X., Tian, X.-Y., Zhang, Y.-B., Fu, X.-J., Zhang, S.-Y., 2021. Discovery of 1,2,4-triazine dithiocarbamate derivatives as NEDDylation agonists to inhibit gastric cancers. *Eur. J. Med. Chem.* 225, 113801.
- Takac, P., Kello, M., Vilkova, M., Vaskova, J., Michalkova, R., Mojzisova, G., Mojzis, J., 2020. Antiproliferative Effect of Acridine Chalcone Is Mediated by Induction of Oxidative Stress. *Biomolecules* 10.
- Xiang, H.Y., Chen, Y.H., Wang, Y., Zhang, X., Ding, J., Meng, L.H., Yang, C.H., 2020. Design, synthesis and antiproliferative activity evaluation of a series of pyrrolo[2,1-f][1,2,4]triazine derivatives. *Bioorg. Med. Chem. Lett.* 30, 127194.
- Zhang, B., Duan, D., Ge, C., Yao, J., Liu, Y., Li, X., Fang, J., 2015. Synthesis of Xanthohumol Analogues and Discovery of Potent Thioredoxin Reductase Inhibitor as Potential Anticancer Agent. *J. Med. Chem.* 58, 1795–1805.
- Zhang, S., Li, T., Zhang, Y., Xu, H., Li, Y., Zi, X., Yu, H., Li, J., Jin, C.-Y., Liu, H.-M., 2016. A new brominated chalcone derivative suppresses the growth of gastric cancer cells in vitro and in vivo involving ROS mediated up-regulation of DR5 and 4 expression and apoptosis. *Toxicol. Appl. Pharmacol.* 309, 77–86.
- Zhang, S., Li, T., Zhang, L., Wang, X., Dong, H., Li, L., Fu, D., Li, Y., Zi, X., Liu, H.M., Zhang, Y., Xu, H., Jin, C.Y., 2017. A novel chalcone derivative S17 induces apoptosis through ROS dependent DR5 up-regulation in gastric cancer cells. *Sci. Rep.* 7, 9873.
- M. Zhu, J. Wang, J. Xie, L. Chen, X. Wei, X. Jiang, M. Bao, Y. Qiu, Q. Chen, W. Li, C. Jiang, X. Zhou, L. Jiang, P. Qiu, J. Wu, Design,

- synthesis, and evaluation of chalcone analogues incorporate  $\alpha,\beta$ -Unsaturated ketone functionality as anti-lung cancer agents via evoking ROS to induce pyroptosis, *Europ. J. Med. Chem.* 157 (2018) 1395-1405.
- Zhu, M., Wang, J., Xie, J., Chen, L., Wei, X., Jiang, X., Bao, M., Qiu, Y., Chen, Q., Li, W., Jiang, C., Zhou, X., Jiang, L., Qiu, P., Wu, J., 2018. Design, synthesis, and evaluation of chalcone analogues incorporate  $\alpha, \beta$ -Unsaturated ketone functionality as anti-lung cancer agents via evoking ROS to induce pyroptosis. *Eur. J. Med. Chem.* 157, 1395–1405.
- Zhuang, C., Zhang, W., Sheng, C., Zhang, W., Miao, Z., 2017. Chalcone: A Privileged Structure in Medicinal Chemistry. *Chem. Rev.* 117, 7762.